JOURNAL OF MATERIALS SCIENCE **35** (2000) 3681 – 3684

Microstructural characterisation of alumina with Ti ion implantation

H. JI
Surface Engineering Research Centre, Department of Materials Engineering, University of Wollongong, NSW 2500, Australia

P. J. EVANS
Physics Division, ANSTO, Menai, NSW 2234, Australia

M. SAMANDI
Surface Engineering Research Centre, Department of Materials Engineering, University of Wollongong, NSW 2500, Australia

The microstructure of alumina after Ti ion implantation has been investigated. A metal vapour vacuum arc (MEVVA) ion source was employed to implant Ti ions into alumina with doses of 7.6×10^{16} and 3.1×10^{17} ions/cm^2 at 40 kV. Scanning electron microscopy (SEM) of the irradiated surfaces revealed topographical changes, which were dependent on dose. The implanted layer was also characterised by Rutherford backscattering (RBS) and cross-sectional transmission electron microscopy (XTEM) which showed the lower Ti dose resulted in a highly defective surface layer. In contrast, TiO_2 precipitates in an amorphous matrix were observed at the higher dose. © *2000 Kluwer Academic Publishers*

1. Introduction

In recent years, there has been increasing interest in the use of ion implantation to alter specific surface properties of a wide range of materials for tribological, electronic and optical applications without the loss of bulk properties. Much of this interest has focussed on the implantation of semiconductors and metals while ceramics have been less studied on account of their complexity. For instance, the microstructure of implanted ceramics is dependent on the chemical and electrical nature of impurities, in addition to the ion energy [1]. Defects produced by ion bombardment are strongly influenced by local stoichiometry and chemical bonding. These defects can induce a crystalline to amorphous transformation in the near surface region. Ion implantation can also lead to the formation of new phases through reaction and recrystallisation. For example, Ti ions implanted into SiO_2 readily interact to form titanium silicides and oxides [2].

Alumina is a common, ionically bonded ceramic used in engineering applications. Substantial damage but no amorphisation was observed in single crystal alumina specimens after implantation of 150 keV Ti ions to a dose of 3×10^{16} ions/cm^2 [3]. The effect of ion implantation on the surface hardness of Al_2O_3 has also been the subject of several studies [4–7]. Variations in this property were attributed to changes in the surface microstructure, which was found to be strongly influenced by ion dose.

Clearly, defects introduced by ion implantation can result in different microstructural modifications to the substrate. Therefore, it is desirable to characterise such changes in ion implanted ceramics in order to understand the mechanism of surface modification resulting from ion bombardment. In the present study, the microstructure of Al_2O_3 was characterised using scanning electron microscopy (SEM), cross-sectional transmission electron microscopy (XTEM) and Rutherford backscattering (RBS).

2. Experiments

The substrate material used for Ti ion implantation was a commercially available high purity alumina (α-Al_2O_3). Specimens (10×10 mm^2) were prepared by grinding and polishing the surface to be implanted to a 1 μm diamond finish. A metal vapour vacuum arc (MEVVA) ion source was employed for the implantations [8, 9]. This type of ion source typically produces a beam containing ions with several charge states [8]. In the case of titanium, Ti^+, Ti^{2+} and Ti^{3+} are extracted from the source yielding an average charge state of 2.1 [10]. Thus, an ion beam with average energy of 84 keV, composed of ions with energies of 40, 80 and 120 keV, was obtained at the extraction voltage of 40 kV used in the present work. Ion doses of 7.6×10^{16} and 3.1×10^{17} ions/cm^2 were implanted into the Al_2O_3 specimens. During implantation, a small area on each sample was masked to provide a reference surface. The base pressure of the implanter was typically $\leq 1 \times 10^{-6}$ Torr with a small increase occurring when the source was operating.

The Ti implanted Al_2O_3 specimens were characterised with Rutherford backscattering (RBS) using a 2.0 MeV $^4He^+$ beam and a backscatter angle of 169°. The surface morphology of selected samples was

examined with scanning electron microscopy (SEM). Transmission electron microscopy (TEM) provided a valuable complement to the other techniques for the characterisation of local microstructural and morphological information and the nature of phase formation sequences in an interaction layer. Thin specimens were prepared by ion beam milling and then examined by TEM on a JEOL 2000 at 200 kV.

3. Results

The RBS spectra of Ti implanted Al_2O_3 with doses of 7.6×10^{16} and 3.1×10^{17} ions/cm^2 at ambient temperature are plotted in Fig. 1 together with the spectrum of an as-polished reference specimen. The increase in the Ti signal as a function of dose and the corresponding decrease in that of aluminium in the near surface region, clearly evident in this figure, are indicative of the displacement of Al by Ti ions due to the implantation. The concentration of implanted Ti retained in Al_2O_3 was determined from the RBS spectra by means of the RUMP program [11]. This yielded peak Ti concentrations of 14 and 50 at.% for ion influences of 7.6×10^{16} and 3.1×10^{17} ions/cm^2 respectively.

The surface topography of unimplanted and Ti implanted Al_2O_3 was examined by SEM as shown in Fig. 2. It can be seen that there was a clear change in the surface following implantation. Compared with the surface of unimplanted Al_2O_3, the imaged region showed clear grain boundaries when Al_2O_3 was bombarded by Ti ions at 7.6×10^{16} ions/cm^2. This suggests that differential grain erosion may occur as a result of ion bombardment. In contrast, the surface of Ti implanted Al_2O_3 became smoother and the grain boundary was no longer visible when the sample was subjected to the higher dose of 3.1×10^{17} ions/cm^2. It is known that a certain level of surface topographic feature will be associated with ion implantation [12]. The free energy state of rough surfaces is higher than that of smooth surfaces. Thus a smoother surface will be produced by the defect fluxes induced by Ti implantation, particularly at the higher dose of 3.1×10^{17} ions/cm^2 and 80 keV average ion energy for Al_2O_3 (cf. Fig. 2b and c).

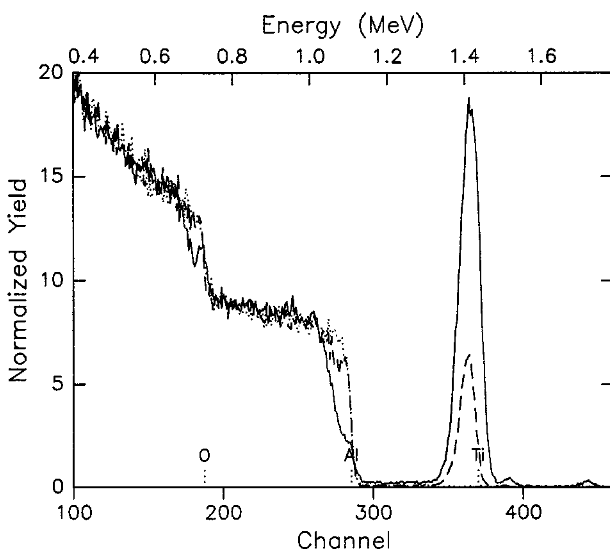

Figure 1 RBS spectra of Al_2O_3 implanted with Ti ions at 7.6×10^{16} ions cm^{-2} (- - - -), 3.1×10^{17} ions cm^{-2} (——) and an as-polished reference specimen (· · · · · ·).

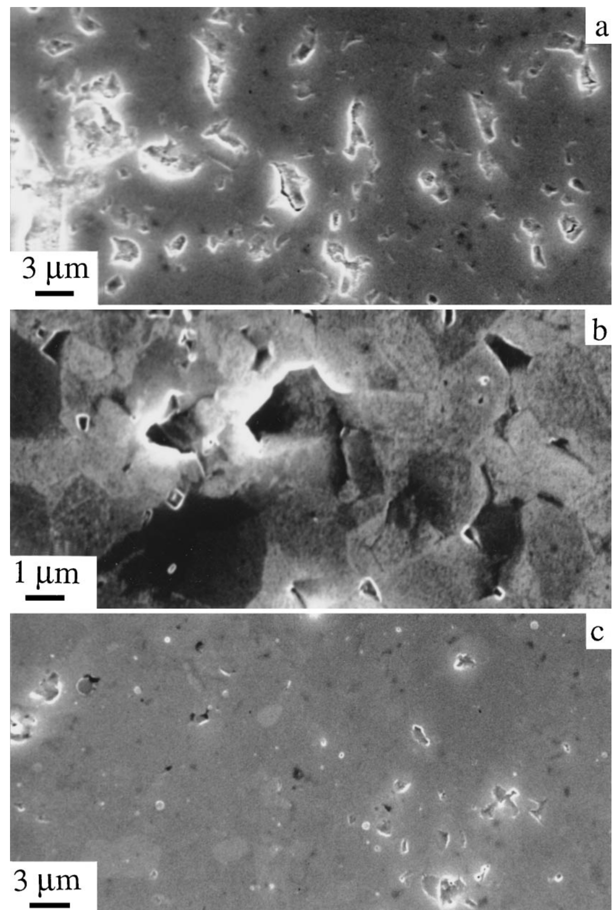

Figure 2 SEM micrographs showing surface of Al_2O_3 before and after implantation: (a) unimplanted, (b) implanted with 7.6×10^{16} ions cm^{-2} and (c) implanted with 3.1×10^{17} ions cm^{-2}.

A cross sectional TEM micrograph of alumina implanted with Ti ions at 7.6×10^{16} ions/cm^2 is shown in Fig. 3. Note that ion implantation has produced a distinct layer extending to a depth of $\sim$100 nm below the sample surface. Such surface layers were not observed in XTEM micrographs of as-polished, unimplanted Al_2O_3. The implantation layer exhibited a high concentration of defects produced by bombardment of Ti ions. These defects were mainly vacancies, interstitials and impurities. Corresponding nano-beam electron diffraction (NBED) patterns of two locations in the Ti implantation layer and Al_2O_3 matrix are given as inserts in Fig. 3. The patterns from the Ti implantation layer were consistent with the hexagonal structure of α-Al_2O_3 in the direction of $[\bar{1}2\bar{1}1]$, identical with the unimplanted Al_2O_3 substrate. This result indicates that the implantation layer is fully monocrystalline with the same orientation as the underlying α-Al_2O_3 grain.

In contrast, Fig. 4 presents a typical TEM micrograph of Ti implanted Al_2O_3 at the higher dose of 3.1×10^{17} ions/cm^2. The implantation layer on the surface of the Al_2O_3 is clearly visible in this image. It is noted that part of Al_2O_3 grain boundary structure has been replaced by a continuous implanted layer. This implanted layer basically comprised two sublayers, denoted on the figure

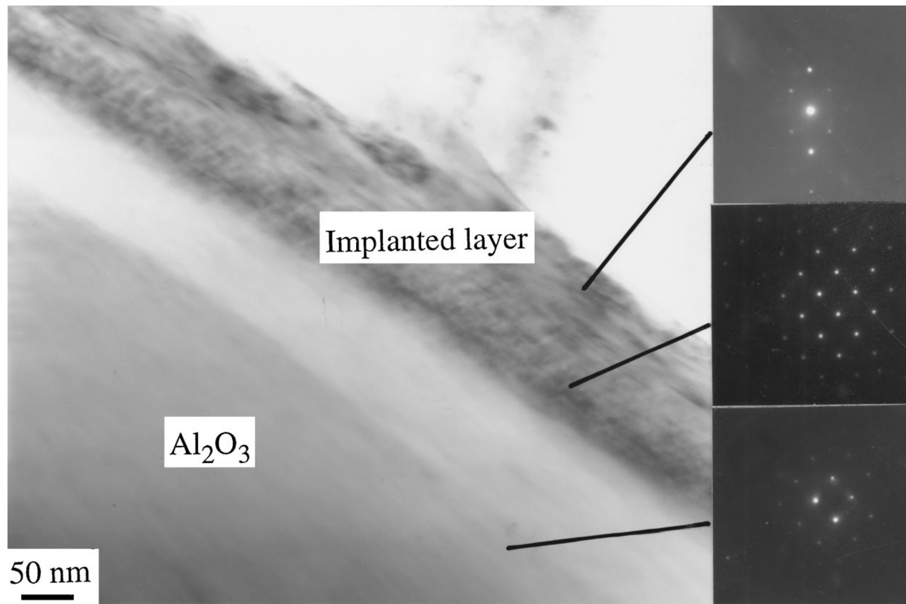

Figure 3 TEM micrograph of Al_2O_3 implanted with a Ti dose of 7.6×10^{16} ions cm^{-2} showing the implantation layer with NBED patterns.

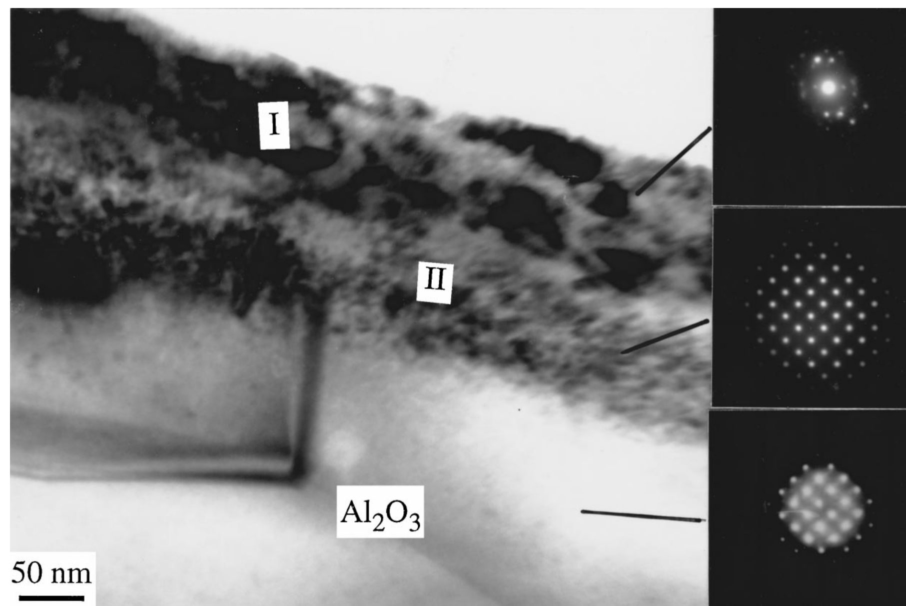

Figure 4 TEM micrograph of Al_2O_3 implanted with a Ti dose of 3.1×10^{17} ions cm^{-2} showing an implantation layer comprising two distinct sublayers with associated NBED patterns.

as regions I and II. Sublayer I, located immediately below the sample surface, was ∼90 nm wide while sublayer II, adjacent to the unmodified alumina, was ∼70 nm wide and contained the higher concentration of defects. The NBED patterns taken from sublayers I and II and the α-Al_2O_3 matrix are also shown in Fig. 4. The pattern from sublayer I showed crystal diffraction spots that made a near crystal ring pattern. This indicates that sublayer I is no longer monocrystalline and predominantly consisted of numerous fine precipitates. It was initially determined to be TiO_2 since the index of the diffraction pattern for this layer was consistent with the structure of TiO_2. Sublayer II exhibited similar features to the Ti implanted layer produced at the lower dose of 7.6×10^{16} ions/cm^2. The diffraction pattern from this region was clearly consistent with that obtained from the α-Al_2O_3 matrix in the direction of [$\bar{4}$401]. Sublayer II remains fully monocrystalline despite the high concentration of defects present in this region. With increasing fluence and hence Ti concentration, precipitation may occur resulting in the formation of a new phase. The TiO_2 detected in the higher dose specimen could be caused by the compositional changes induced by implantation of Ti. Furthermore, the high density of defects may have promoted the growth of such precipitates [12].

4. Discussion

The experimental results obtained by RBS and electron microscopy in conjunction with electron diffraction have shown the microstructural development of Ti implanted Al_2O_3 from low dose to high dose. A model, based on the accumulation of defects, provides

an explanation of structural changes induced by ion implantation [13]. During implantation, atoms of the Al_2O_3 target can be displaced through collisions with incident ions of sufficient energy. This process produces a cascade of recoiling atoms, which results in the formation of defects, such as vacancies, interstitials and impurities. These defects will be accumulated and rearranged into a metastable configuration as the ion fluence is increased. Consequently, the long range order of the crystal lattice is destroyed and an amorphous state is produced if a critical defect concentration is reached [14].

In the case of Ti implanted Al_2O_3 at low dose, it has been noted that the implanted surface presented clear grain boundaries etched by ion bombardment and the implanted layer retained the α-Al_2O_3 structure although a considerable number of defects were evident. The change in the structure of the implanted layer is strongly dependent upon the damage left after dynamic recovery processes annihilate most of the defects produced in the collision cascade. The depth of amorphization will be associated with incident ion flux and energy [15]. At high dose, the higher concentration of titanium implanted in the modified layer produced a higher density of defects and more damage. Titanium has high affinity for oxygen and preferentially reacts with it to form titanium oxide when it is implanted into alumina. It is likely that the high Ti concentration led to the formation of a new phase that developed as fine precipitates [16]. Therefore, precipitation of titanium oxide from the amorphous state would take place when some threshold concentration of Ti, corresponding to a dose $< 3.1 \times 10^{17}$ ions/cm^2, was implanted. The development of microstructure associated with this process will lead to the change in the surface topography of Ti implanted Al_2O_3 as observed above.

5. Conclusion

The microstructure of Ti implanted Al_2O_3 at both low and high doses has been investigated by electron microscopy. The near surface of Ti implanted Al_2O_3 was modified by Ti ion bombardment and the resulting change in microstructure was associated with ion fluence. No evidence of amorphisation was revealed, as Al_2O_3 is an ionically bonded ceramic which requires high implantation energy and high fluence for amorphisation. Based on the electron diffraction data, it appears likely that fine precipitates of TiO_2 are produced at the higher dose studied.

Acknowledgement

The award of a grant by the Australian Institute of Nuclear Science and Engineering (AINSE) in partial support of this work is gratefully acknowledged.

References

1. C. J. McHargue, *Nucl. Instrum. Methods* **B19/20** (1994) 797.
2. J. S. Daniel, P. Martin, M. Dufour, A. Ermolieff, S. Marthon, F. Pierre and M. Dupuy, 1993 IEEE International Frequency Control Symposium, 1993, p. 597.
3. H. Naramoto, C. J. McHargue, C. W. White, J. M. Williams, O. W. Holland, M. M. Abraham and B. R. Appleton, *Nucl. Instrum. Methods* **B209/210** (1983) 1159.
4. C. J. McHargue, G. C. Farlow, C. W. White, J. M. Williams, P. Angelini and G. M. Begun, *Mater. Sci. Eng.* **69** (1985) 123.
5. F. Halitim, S. Paletto, G. Fantozzi and D. Treheux, *J. Eur. Ceramic Soc.* **15** (1995) 833.
6. S. M. M. Ramos, B. Cannt, L. Gea, P. Thevenard, M. Bauer, Y. Maheo, P. Kapsa and J. L. Loubet, *J. Mater. Res.* **7** (1992) 178.
7. F. Halitim, N. Ikhlef, L. Boudoukha and G. Fantozzi, *J. Phys. D* **30** (1997) 330.
8. I. G. Brown, J. E. Galvin, B. F. Gavin and R. A. MacGill, *Rev. Sci. Instrum.* **57** (1986) 1069.
9. R. Cornelius, M. Samandi and P. J. Evans, *Surface Eng.* **11** (1995) 123.
10. I. G. Brown and X. Godechot, *IEEE Trans. Plasma Sci.* **19** (1991) 713.
11. L. Doolittle, *Nucl. Instrum. Methods* **B9** (1985) 334.
12. A. Rahioui and C. Esnouf, *Surface & Coating Tech.* **45** (1991) 23.
13. R. Kelly, in "Beam Modification of Materials 1," edited by O. Auciello and R. Kelly (Elsevier, Netherlands, 1984) p. 79.
14. O. Auciello, R. Kelly and R. Iricibar, *Rad. Effects* **46** (1980) 105.
15. R. Kelly and N. Q. Lam, *Rad Effects* **10** (1971) 247.
16. P. D. Townsend, in "Materials and Processes for Surface and Interface Engineering," edited by Y. Pauleau (Kluwer, Netherlands, 1995) p. 285.

Received 3 April 1998
and accepted 3 February 2000